INSTITUTE OF PHYSICS PUBLISHING PHYSICS IN MEDICINE AND BIOLOGY

Phys. Med. Biol. **48** (2003) 1361–1370 PII: S0031-9155(03)58944-8

Effects of anisotropic optical properties on photon migration in structured tissues

Leonardo Dagdug[1], George H Weiss[1] and Amir H Gandjbakhche[2]

[1] Mathematical and Statistical Computing Laboratory, Center for Information Technology, Bethesda, MD 20892-5626, USA

[2] Laboratory of Integrative and Medical Biophysics, Institute of Child Health and Human Development, National Institutes of Health, Bethesda, MD 20892, USA

Received 30 January 2003
Published 7 May 2003
Online at stacks.iop.org/PMB/48/1361

Abstract

It is often adequate to model photon migration in human tissue in terms of isotropic diffusion or random walk models. A nearly universal assumption in earlier analyses is that anisotropic tissue optical properties are satisfactorily modelled by using a transport-corrected scattering coefficient which then allows one to use isotropic diffusion-like models. In the present paper we introduce a formalism, based on the continuous-time random walk, which explicitly allows the diffusion coefficients to differ along the three axes. The corrections necessitated by this form of anisotropy are analysed in the case of continuous-wave and time-resolved measurements and for both reflectance and transmission modes. An alternate model can be developed in terms of a continuous-time random walk in which the times between successive jumps differ along the three axes, but is not included here.

(Some figures in this article are in colour only in the electronic version)

1. Introduction

Diffusion-like theories are frequently used to describe photon migration in biological tissues (Gandjbakhche and Weiss 1995). The terminology ‘diffusion’ will refer to standard diffusion theory as well as to the discrete analogue of diffusion theory, namely lattice random walk theory. While such theories cannot be applied to reduce data taken at very short times, there is a large body of data in which diffusion theory is appropriate and provides a description of photon migration sufficiently accurate for practical applications. This is true regardless of the particular variety of the optical measurements, i.e., transmittance, reflectance or tomographic, and the specific type of measurement, i.e., time-gated, CW, or in the frequency-domain. Because of the simplicity of diffusion or random walk theory a phenomenological way of incorporating anisotropic scattering is to correct the intrinsic scattering coefficient μ_s by using the modified scattering coefficient $\mu_s' = \mu_s(1 - \langle\cos\theta\rangle)$ where $\langle\cos\theta\rangle$ is the mean scattering angle. The scattering coefficient μ_s' is then used to define the diffusion constant to be used in an isotropic version of the theory.

While most body tissues can be quite accurately described as having transport-corrected isotropic optical properties, there are some in which directionality of the constituent fibres cannot be ignored. Among these are skin (Nickell *et al* 2000), white matter in brain, collagen and dentin (Kienle *et al* 2003). Simon Arridge at University College, London, and his collaborators at the University of Helsinki were the first research group to address this problem in some generality and study its implications in the context of diffuse optical tomography (Heino *et al* 2002). In their investigation they replace the scalar value of the anisotropy coefficient by a tensor describing the direction of photon diffusion in the tissue. In the present paper we develop a simplified lattice random walk model which models directional tissue properties in terms of differing transition probabilities along the three axes. This is done to demonstrate how results obtained from the standard isotropic version of the theory are qualitatively modified by the degree of anisotropy. A theory along the same lines is presently being developed in which the degree of anisotropy is allowed to be more general than that considered in the present paper.

To facilitate the analysis we make use of a modification of the continuous-time random walk (CTRW) (Weiss 1994), as first applied to optical problems in Weiss *et al* (1998). The CTRW is a random walk on a simple cubic lattice in which the times between successive steps are themselves random variables. In the present context the advantage of using the CTRW is that it avoids certain singularities which arise when the analysis based on a Gaussian approximation is used. In the investigation by Weiss *et al* (1998) the lattice was assumed to have isotropic optical properties. In the present analysis we relax this assumption, allowing transition probabilities along the different axes to differ. The present model is analysed in a simplified form in which the axes are restricted to be parallel to those of the laboratory reference frame.

We point out that, in the framework of the CTRW, there are at least two ways in which deviations from complete isotropy can be modelled. The first is that the transition probabilities can be made to depend on the axis direction, and the second is one in which the probability density for interjump intervals is allowed to differ, depending on the chosen axis along which the random walker moves. In this paper we study only the effects of the first of these possibilities. Two geometries will be considered, one in which the tissue is regarded to be a semi-infinite medium bounded by a planar surface, and the second, in which the tissue is modelled as a slab bounded by two planar surfaces.

2. Definition of the model

An arbitrary point in the lattice will be denoted by $\mathbf{r} = (x, y, z)$ where the components x, y and z are integers. The variables x and y are unbounded in both the semi-infinite medium and the slab. In both cases $z = 0$ is assumed to be an absorbing plane while values with $z > 0$ represent points interior to the tissue. In the case of a slab, which models the transillumination measurement, the second absorbing surface is set at $z = L$. Later, the transformation between these dimensionless units and physical units will be cited.

The CTRW model is a random walk in which the times between successive steps are random variables. We deal with the simplest example of a CTRW which has the advantage of allowing results to be expressed in a closed form. This is defined by the probability density for the interjump times being

$$\psi(t) = k\mathrm{e}^{-kt}. \tag{2.1}$$

The following analysis will be expressed in terms of the dimensionless time $\tau = kt$, which is equivalent to setting $k = 1$. We also use the assumption that photons may be absorbed internally, the absorption following the Beer–Lambert law. The dimensionless absorption coefficient will be denoted by ν so that the probability that a photon survives for a time τ without being absorbed is $e^{-\nu\tau}$. If we further restrict the random walk to make steps to nearest-neighbouring sites only, then the propagator for an isotropic random walk in free space, i.e., the probability that the random walk is at $\mathbf{r}$ at time τ, has been shown to be

$$p^{(F)}(\mathbf{r}, \tau|\mathbf{r}_0) = e^{-(1+\nu)\tau} I_{x-x_0}\left(\frac{\tau}{3}\right) I_{y-y_0}\left(\frac{\tau}{3}\right) I_{z-z_0}\left(\frac{\tau}{3}\right) \tag{2.2}$$

where $\mathbf{r}_0 = (x_0, y_0, z_0)$ is the initial position of the random walker and $I_m(u)$ is a modified Bessel function of the first kind (Weiss *et al* 1998). The propagator in the presence of planar absorbing boundaries can be found in terms of $p^{(F)}(\mathbf{r}, \tau|\mathbf{r}_0)$ by utilizing the method of images (Riley *et al* 2002).

To define an analogue to equation (2.2) incorporating directionality we retain the simple cubic lattice structure of the tissue, but now assume that in a given step the choice of axis along which it is made is no longer equal to $1/3$ as in the case of isotropy. Rather, we will assume that the x-axis is chosen for a given step, with probability α, the y-axis with probability β and the z-axis with probability γ. It is further assumed that the random walk along each of the axes is symmetric. That is to say, the probability of making a step $z \to z + 1$ is equal to that of making the step $z \to z - 1$, both being equal to γ. With these definitions, the transition probabilities satisfy the condition

$$2\alpha + 2\beta + 2\gamma = 1. \tag{2.3}$$

For simplicity we analyse only two special cases: $\alpha = \beta \neq \gamma$ and $\beta = \gamma \neq \alpha$. The first of these is a case in which there is radial symmetry in any (x, y) plane with a possibly different transition probability for motion parallel to the z-axis. The second case has the anomalous axis parallel to either the x- or y-axis.

3. The semi-infinite medium

3.1. Longitudinal directionality

In the most general case the free-space propagator in equation (2.2) is replaced by

$$p^{(F)}(\mathbf{r}, \tau|\mathbf{r}_0) = e^{-(1+\nu)\tau} I_{x-x_0}(2\alpha\tau) I_{y-y_0}(2\beta\tau) I_{z-z_0}(2\gamma\tau) \tag{3.1}$$

which is derived exactly as in Weiss *et al* (1998) and which reduces to the isotropic result when $\alpha = \beta = \gamma = 1/6$. In all cases the initial position is set at $\mathbf{r}_0 = (0, 0, 1)$ so that the propagator for the semi-infinite tissue in the presence of an absorbing plane is found by the method of images to be

$$\begin{aligned} p(\mathbf{r}, \tau|\mathbf{r}_0) &= e^{-(1+\nu)\tau} I_x(2\alpha\tau) I_y(2\beta\tau)[I_{z-1}(2\gamma\tau) - I_{z+1}(2\gamma\tau)] \\ &= z e^{-(1+\nu)\tau} I_x(2\alpha\tau) I_y(2\beta\tau) I_z(2\gamma\tau)/(\gamma\tau) \end{aligned} \tag{3.2}$$

which obviously vanishes at $z = 0$.

We specialize now to the case $\alpha = \beta$ so that the transition probability parallel to the z-axis differs from that in any plane transverse to it. We present results in terms of a bias parameter B, defined by

$$B = \gamma/\alpha \tag{3.3}$$

so that in an isotropic system $B = 1$. Combining the definition of B with equation (2.3) we find that the transition probabilities can be written entirely in terms of the bias parameter as

$$\alpha = \beta = \frac{1}{2B+4} \qquad \gamma = \frac{B}{2B+4}. \tag{3.4}$$

The observable physical quantity in a time-gated measurement is the intensity at $\mathbf{R} = (X, Y, 0)$ at time τ. For a random walk to reach the surface at that location at that time it must be at $(X, Y, 1)$ at τ and make a step at that time to the boundary with probability γ. This leads to an expression for the intensity, $I(\mathbf{R}, \tau)$, which is

$$I(\mathbf{R}, \tau) = \frac{\mathrm{e}^{-(1+\nu)\tau}}{\tau} I_X\left(\frac{\tau}{B+2}\right) I_Y\left(\frac{\tau}{B+2}\right) I_1\left(\frac{B\tau}{B+2}\right). \tag{3.5}$$

If we regard this as a function of B then it follows from this expression that

$$\lim_{B\to 0} I(\mathbf{R}, \tau) = 0 \qquad \lim_{B\to\infty} I(\mathbf{R},\tau) = 0 \tag{3.6}$$

where the last limit on the right-hand side is valid except at the origin $X = Y = Z = 0$. These results are readily interpreted. The condition $B = 0$ restricts motion to be parallel to the absorbing plane so that the random walk can never reach the absorbing plane. When $B = \infty$ only motion along the z-axis is allowed so that the random walk can only escape at $\mathbf{R} = \mathbf{0}$. Hence, in this case, the intensity on the surface is zero except at the origin.

To discuss directionality effects we transform an approximation to the propagator so that the constants can all be written in terms of the bias. At sufficiently long times equation (3.2) approaches a damped Gaussian, which one finds by making use of the large-ξ approximation

$$\mathrm{e}^{-\xi} I_x(\xi) \approx \frac{1}{\sqrt{2\pi\xi}} \exp\left(-\frac{x^2}{2\xi}\right). \tag{3.7}$$

As a result, the propagator at long times is approximately Gaussian, having the form

$$p(\mathbf{r}, \tau|\mathbf{r}_0) \approx \frac{z}{8\alpha(\pi\gamma)^{3/2}\tau^{5/2}} \exp\left\{-\frac{\gamma\rho^2 + \alpha z^2}{4\alpha\gamma\tau} - \nu\tau\right\} \tag{3.8}$$

where $\rho^2 = x^2 + y^2$. A transformation using equation (3.4) yields an equivalent formula in terms of the bias B:

$$p(\mathbf{r}, \tau|\mathbf{r}_0) \approx \frac{(B+2)^{3/2} z}{\sqrt{8\pi^3 B\tau^5}} \exp\left\{-\left(1 + \frac{B}{2}\right)\left(\rho^2 + \frac{z^2}{B}\right)\frac{1}{\tau} - \nu\tau\right\}. \tag{3.9}$$

With this expression in hand it is possible to find a long-time approximation to the light intensity at the detection point $\mathbf{R}$ in a time-gated measurement. We can appeal to the expression for the intensity given in equation (3.5) to find the approximation

$$\begin{aligned} I(\mathbf{R}, \tau) &\approx \frac{1}{2\pi^{3/2}(1-2\gamma)\gamma^{1/2}\tau^{5/2}} \exp\left\{-\frac{4\gamma\rho^2 + 1 - 2\gamma}{4\gamma(1-2\gamma)\tau} - \nu\tau\right\} \\ &= \frac{(B+2)^{3/2}}{(2\pi)^{3/2}B^{1/2}\tau^{5/2}} \exp\left[-\left(\frac{B}{2} + 1\right)\left(\rho^2 + \frac{1}{B}\right)\frac{1}{\tau} - \nu\tau\right]. \end{aligned} \tag{3.10}$$

When $B = 1$ this expression for $I(\mathbf{R}, \tau)$ reproduces an expression for the intensity originally given in Bonner *et al* (1987).

Figure 1 shows curves of $I(\mathbf{R}, \tau)$ as a function of τ for $\rho = 3$ and three values of B. The time at which the peak occurs is seen to increase as B increases in this particular example. This, however, is not a general result, but depends on the value of ρ. It is easy to evaluate the

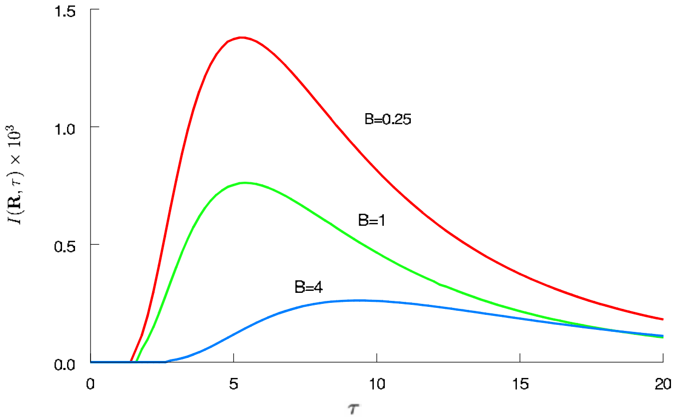

Figure 1. The time-dependent behaviour of the intensity in a time-gated measurement at $\rho = 2$ plotted as a function of time for different values of the bias parameter B. As the value of B increases, the maximum value of the intensity is also seen to increase as well as the time at which the maximum occurs.

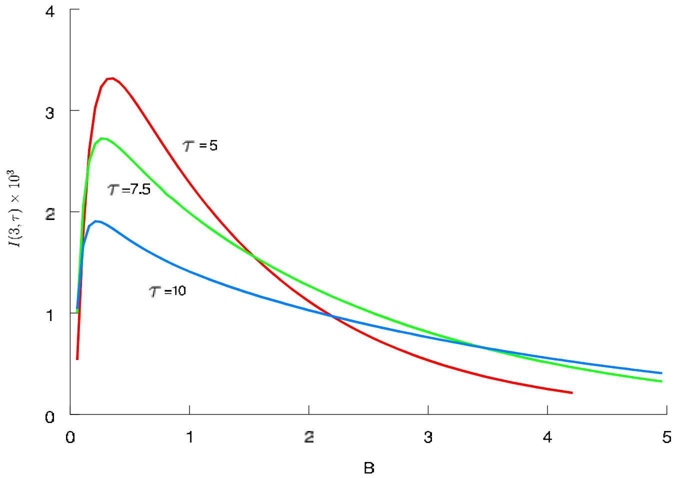

Figure 2. Curves of $1000I(3, \tau)$ plotted as a function of the bias parameter B at three values of the time. The salient features of the curves are the maximum at small B at the shortest value of the time. At larger values of the bias, B, the contribution from longer times predominates.

time at which the peak occurs, $\tau_{\max}(B, \rho)$, from the expression for $I(\mathbf{R}, \tau)$ in equation (3.10). It is

$$\tau_{\max}(B, \rho) = \frac{5}{2}\left[\sqrt{1 + \frac{16\nu\left(\frac{B}{2}+1\right)\left(\rho^2+\frac{1}{B}\right)}{25}} - 1\right]. \tag{3.11}$$

This is a monotonically increasing function of the distance to the target radius, ρ, reflecting the obvious fact that the photon requires a longer time to arrive at the absorbing plane as ρ increases. It is also an increasing function of the absorption parameter ν, but not of the parameter B since $\tau_{\max}(0, \rho) = \tau_{\max}(\infty, \rho) = \infty$.

Figure 2 shows three curves of the intensity plotted as $1000I(\mathbf{R}, \tau)$ and calculated from equation (3.10). The curves, which correspond to $\rho = 3$, are plotted as a function of the bias parameter B for three values of the time, τ. Two qualitative features are evident from the figure. The first is that at relative small values of B the short term photons predominate in contributing to the surface intensity, and the second is that at larger values of B the longer time photons are the major contributors to the surface intensity. A simple physical argument can be given for these results. When B is relatively small, photons tend to spread out in the plain $z = 1$, from which a few will reach the surface at a short distance from the entry point. On the other hand, as B is increased, the random walkers tend to cluster around $x = y = 0$ and only a few photons will reach the surface at $\rho = 3$, taking a long time to do so. The intensity is also attenuated at the larger values of B, an effect attributable to the effects of internal absorption.

In the CW experiment the intensity as a function of the parameters is found by integrating $I(\mathbf{R}, \tau)$ over all τ. The result of doing so gives a result that can be written as

$$I(\rho) = \int_0^\infty I(\mathbf{R}, \tau)\,\mathrm{d}\tau \approx \frac{\sqrt{2\nu B(B+2)}}{8\pi E(\rho)}\left(1 + \frac{1}{\sqrt{4\nu E(\rho)}}\right)\mathrm{e}^{-\sqrt{4\nu E(\rho)}} \tag{3.12}$$

in which

$$E(\rho) = \left(1 + \frac{B}{2}\right)(\rho^2 + 1). \tag{3.13}$$

This reduces to the isotropic result when $B = 1$.

3.2. Directionality parallel to the interface

So far our analysis has described qualitative features of a situation in which measurements are made along the fibre, while radial symmetry is preserved in any plane perpendicular to that fibre. We therefore consider a similar analysis when anisotropy is due to tubules parallel to the face of the tooth and measurements are made perpendicular to that face as in the study by Kienle *et al* (2003). This can be defined more precisely by setting $\alpha = \gamma \neq \beta$. Since now the anomalous parameter is β rather than γ we define a new bias parameter as $B' = \beta/\gamma$. The transition probabilities are written in terms of the bias parameter as

$$\alpha = \gamma = \frac{1}{2B' + 4} \qquad \beta = \frac{B'}{2B' + 4}. \tag{3.14}$$

Equation (3.2) for the propagator remains valid for this definition of isotropy. In the Gaussian approximation the analog of equation (3.10), expressed in terms of the anomalous probability β or B', becomes

$$\begin{aligned} I(\mathbf{R}, \tau) &\approx \frac{\exp\left[-\dfrac{4\beta(1 + X^2) + (1 - 2\beta)Y^2}{4\beta(1 - 2\beta)\tau} - \nu\tau\right]}{2(1 - 2\beta)\beta^{1/2}\pi^{3/2}\tau^{5/2}} \\ &= \frac{(B' + 2)^{3/2}}{(2\pi)^{3/2}(B')^{1/2}\tau^{5/2}} \exp\left[-\left(\frac{1}{B'} + \frac{1}{2}\right)(B'(1 + X^2) + Y^2)\frac{1}{\tau} - \nu\tau\right]. \end{aligned} \tag{3.15}$$

The value of $I(\mathbf{R}, \tau)$ goes to zero when β reaches its maximum value of $1/2$ (i.e., $B' = \infty$) since the photon, in this case can only move parallel to the interface and therefore can never reach the surface.

If we examine the expression for $I(\mathbf{R}, \tau)$ in equation (3.15) we see that it has a single peak when regarded as a function of τ. If we set

$$A(\boldsymbol{\rho}) = \left(\frac{1}{B'} + \frac{1}{2}\right)(B'(1 + X^2) + Y^2)\frac{1}{\tau} \tag{3.16}$$

then, provided that ν is small, the approximate peak maximum of $\tau(X, Y)$ occurs at

$$\tau_{\max}(X, Y) \approx 2A(\boldsymbol{\rho})/5. \tag{3.17}$$

One sees that this simply replaces the factor ρ^2 that appears in equation (3.13) by a more general quadratic form in X and Y which accounts for directionality. The lowest order correction to equation (3.17) is proportional to ν. At very large values of $\nu\, \tau_{\max}(X, Y)$ is approximately proportional to $\nu^{1/2}$.

It is interesting to consider the behaviour of $\tau_{\max}(X, Y)$ as a function of B'. A glance at (3.16) indicates that $\tau_{\max}(X, Y)$ is infinite when $B' = 0$ because this restricts the motion to be parallel to the z-axis. Such motion is equivalent to a random walk in one dimension, so that the time to reach the absorbing plane is infinite (Weiss 1994). Equation (3.15) is valid for time-gated measurements. The analogous result for CW measurements is found from equation (3.8) to be

$$I(\boldsymbol{\rho}) = \int_0^\infty I(\boldsymbol{\rho}, \tau)\, \mathrm{d}\tau = \frac{1}{\pi}\sqrt{\frac{\nu}{2}}\left(1 + \frac{2}{B'}\right)^{3/2} \frac{1}{A(\boldsymbol{\rho})}\left(1 + \frac{1}{2\sqrt{\nu A(\boldsymbol{\rho})}}\right) \mathrm{e}^{-2\sqrt{\nu A(\boldsymbol{\rho})}} \tag{3.18}$$

which is similar in form to equation (3.12) except for the replacement of the function $E(\rho)$ by $A(\boldsymbol{\rho})$. Thus, a measurement of surface intensity as a function of the distance in different directions can provide a test for deviation from purely isotropic optical properties, since, when directionality is significant, profiles of the surface intensity will be elliptical rather than circular.

3.3. Mean transit time

A useful parameter which may be used to characterize the average path length in a time-resolved measurement is the average time to reach a distance ρ from the injection point. The mean time to reach $\boldsymbol{\rho} = (X, Y)$ will be denoted by $\langle \tau(\boldsymbol{\rho})\rangle$ and is defined by

$$\langle \tau(\boldsymbol{\rho})\rangle = \frac{\int_0^\infty \tau I(\boldsymbol{\rho}, \tau)\, \mathrm{d}\tau}{\int_0^\infty I(\boldsymbol{\rho}, \tau)\, \mathrm{d}\tau}. \tag{3.19}$$

In the following analysis the integrals will be evaluated in terms of the approximate Gaussian functions in equations (3.10) and (3.15). The parameter $\langle \tau(\boldsymbol{\rho})\rangle$ can be regarded as a measure of the path length of a detected photon provided that the photon is assumed to move at a constant speed through the tissue.

Consider first the case of directionality perpendicular to the interface, i.e., $\alpha = \beta$. An evaluation of $\langle \tau(\boldsymbol{\rho})\rangle$ indicates that it can be expressed in terms of the parameter $E(\boldsymbol{\rho})$, defined in equation (3.13), as

$$\langle \tau(\boldsymbol{\rho})\rangle \approx \frac{2E(\rho)}{1 + 2\sqrt{\nu E(\rho)}}. \tag{3.20}$$

When ρ is large this expression approaches proportionality to the first power of the distance, the specific relation being

$$\langle \tau(\boldsymbol{\rho})\rangle \approx \rho\sqrt{\frac{B+1}{2\nu}}. \tag{3.21}$$

When properties of the medium are isotropic $\langle \tau(\boldsymbol{\rho})\rangle$ was also shown to be proportional to $\rho/\sqrt{\nu}$ in Bonner *et al* (1987). Our present result reduces to that case when $B = 1$.

When directionality is parallel rather than perpendicular to the interface, the relation analogous to equation (3.20) replaces the parameter $E(\rho)$, defined in equation (3.13), by the parameter $A(\boldsymbol{\rho})$ defined in equation (3.16). The model in this case is no longer radially symmetric around the z-axis. When A is large the analogue to equation (3.21) is

$$\langle \tau(\boldsymbol{\rho})\rangle \approx \sqrt{\frac{(B' + 2)[B'(1 + X^2) + Y^2]}{2B'}}. \tag{3.22}$$

Since X and Y have different coefficients in general, this gives the deviation from radial symmetry provided that $B' \neq 1$.

While the formulae mentioned so far have been expressed in terms of dimensionless coordinates these are readily converted to physical coordinates. The dimensionless coordinate $\mathbf{r}$ is converted to the physical coordinate $\mathbf{r}_\mathrm{p}$ by invoking the relation $\mathbf{r}_\mathrm{p} = \mathbf{r}\sqrt{2}/\mu_s'$ where μ_s' is the transport-corrected scattering coefficient (Gandjbakhche *et al* 1992, 1993) while the dimensionless dissipation parameter can be expressed in terms of the absorption and scattering coefficients by the relation $\nu = \mu_a/\mu_s'$ where μ_a is the absorption coefficient.

4. Transillumination measurements

To analyse directionality effects that appear in transillumination measurements it is necessary to have in hand an expression for a propagator in a slab bounded by two parallel absorbing planes, $z = 0$ and $z = L$. This has been calculated for the isotropic case, i.e., when there is no directionality in Weiss *et al* (1998). The analysis is again based on the method of images. A slight modification of that calculation to take into account the slab geometry produces the result

$$p(\mathbf{r};\tau|\mathbf{r}_0) = \frac{2}{L}\,\mathrm{e}^{-(1+\nu)\tau} I_x(2\alpha\tau) I_y(2\beta\tau) \sum_{n=1}^{L-1} \mathrm{e}^{2\gamma\tau\cos(n\pi/L)} \sin\left(\frac{n\pi}{L}\right)\sin\left(\frac{n\pi z}{L}\right) \tag{4.1}$$

when the initial is position $\mathbf{r}_0 = (0, 0, 1)$. In a transillumination measurement the input and output points are $\mathbf{r}_0 = (0, 0, 1)$ and $\mathbf{r}_\mathrm{f} = (0, 0, L)$ respectively. Consequently, the intensity measured at $(0, 0, L)$ at time τ is

$$I(\mathbf{r}_\mathrm{r};\tau) = \gamma p(0, 0, L-1;\tau|\mathbf{r}_0). \tag{4.2}$$

When the directionality is longitudinal, so that the transition probabilities are those given in equation (3.4), $I(\mathbf{r}_\mathrm{r};\tau)$ is given by

$$I(\mathbf{r}_\mathrm{r};\tau) = \frac{B I_0^2\left(\frac{\tau}{B+2}\right)}{L(B+2)} \sum_{n=1}^{L-1} (-1)^{n+1}\,\mathrm{e}^{-a_n\tau} \sin^2\left(\frac{\pi n}{L}\right). \tag{4.3}$$

The parameter a_n used in the sum is given by

$$a_n = 1 + \nu - \frac{B\cos(n\pi/L)}{B+2}. \tag{4.4}$$

The probability density for the time of arrival at $\mathbf{r}_\mathrm{f}$ is given by

$$f(\mathbf{r}_\mathrm{f};\tau) = \frac{I(\mathbf{r}_\mathrm{r};\tau)}{\int_0^\infty I(\mathbf{r}_\mathrm{r};\tau)\,\mathrm{d}\tau} \tag{4.5}$$

where the denominator, evaluated from equation (4.3), is found to be

$$\int_0^\infty I(\mathbf{r}_\mathrm{r};\tau)\,\mathrm{d}\tau = \frac{2B}{\pi L(B+2)} \sum_{n=1}^{L-1} (-1)^{n+1} \sin^2\left(\frac{\pi n}{L}\right) \frac{1}{a_n} K\left(\frac{2}{(B+2)a_n}\right) \tag{4.6}$$

in which $K(k)$ is a complete elliptic integral of the first kind (Magnus *et al* 1966). It is possible to evaluate $\langle\tau(\boldsymbol{\rho})\rangle$ in a closed form for time-gated measurements with off-axis points $\mathbf{r}_\mathrm{f} = (X, Y, 0)$, provided that the Gaussian approximation in equation (3.7) is valid. The result is quite complicated, and is therefore omitted from the present exposition.

Typical plots of the function $f(\mathbf{r}_\mathrm{f};\tau)$ as calculated from equations (4.5) and (4.6) are shown in figure 3. The curves in this figure indicate that the larger the bias the shorter is the time for the random walker to be trapped at the point opposite to the input optode. The curves

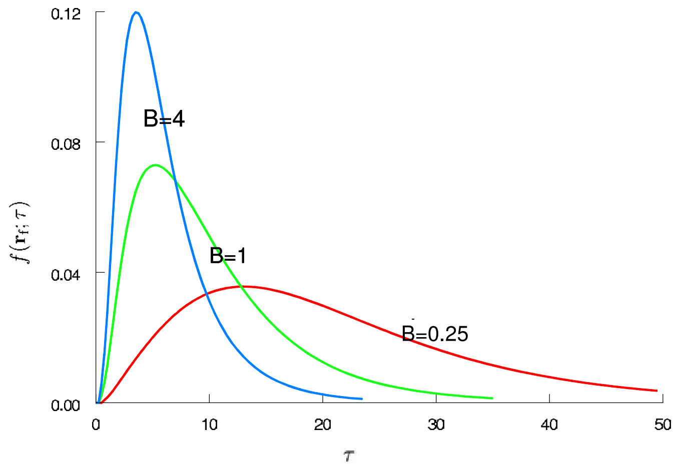

Figure 3. Three curves of the function $f(\mathbf{r}_f; \tau)$ as defined in equation (4.5) as a function of τ and for three values of transverse bias. The curves were generated for $L = 5$ and $\nu = 0.05$. Note that increasing the value of ν is equivalent to increasing the time spent by the photon in moving in the z-direction, which, in effect, filters out those photons which take longer times to reach the site at which they are absorbed.

in figure 3 were generated for the value $\nu = 0.05$. When this absorption parameter increases the time of arrival at the trapping point will decrease, i.e., the curves shown will sharpen up and the value of $\mathbf{r}_f$ at which $f(\mathbf{r}_f; \tau)$ is a maximum will decrease. This occurs because only those photons that move so as to minimize their time of exposure to absorption will have a chance to reach the target point.

5. Concluding remarks

Our analysis in this paper is based on a continuous-time lattice random walk on either a semi-infinite medium bounded by a plane or a slab. The CTRW formalism allows us to derive at least some results in explicit form in the time domain and can be shown to be equivalent to the Gaussian approximation at large distances from the input point. We have aimed at deriving qualitative features of photon migration in media whose optical properties are non-isotropic. To simplify the analysis we have also restricted it to media in which the directional properties are parallel to the coordinate axes. A more comprehensive analysis based on an arbitrary orientation of directional properties with respect to the laboratory coordinate system can be developed, but is not done here. An experimentally measurable parameter has been suggested and analysed in the present work, that is, the mean time to reach a given site. Approximations to this parameter have been given in equation (3.20) for the semi-infinite medium.

Finally, other parameters are available to characterize trajectories in a directional medium, exemplified by the mean depth reached by a photon, conditional on its reaching the surface, as discussed in Bonner *et al* (1987) for the isotropic medium. This parameter would obviously be sensitive to directional properties.

Acknowledgment

We are grateful to Dr Alexander Berezhkovskii for a useful discussion.

References

Bonner R F, Havlin S, Nossal R and Weiss G H 1987 Model for photon migration in turbid biological media *J. Opt. Soc. Am.* A **4** 423–32

Gandjbakhche A H, Bonner R F and Nossal R 1992 Scaling relationships for anisotropic random walks *J. Stat. Phys.* **46** 35–53

Gandjbakhche A H, Nossal R and Bonner R F 1993 Scaling relationships for theories of anisotropic random walks applied to tissue optics *Appl. Opt.* **32** 504–16

Gandjbakhche A H and Weiss G H 1995 Random walk and diffusion-like models of photon migration in turbid media *Prog. Opt.* **34** 335–402

Heino J, Arridge S and Sommersalo E 2002 Anisotropic effect in light scattering and some implications in optical tomography *Tech. Dig. OSA Biomedical Topical Meetings* pp 18–20

Kienle A, Forster F K, Diebolder R and Hibst R 2003 Light propagation in dentin: influence of microstructure on anisotropy *Phys. Med. Biol.* **48** N7–N14

Magnus W, Oberhettinger F and Soni R P 1966 *Formulas and Theorems for the Special Functions of Mathematical Physics* (New York: Springer)

Nickell S, Herrman M, Ehrenpreis M, Farrell T J, Krämer U and Patterson M S 2000 Anisotropy of light propagation in human skin *Phys. Med. Biol.* **45** 2873–86

Riley K F, Hobson M P and Bence S J 2002 *Mathematical Methods for Physics and Engineering* 2nd edn (Cambridge: Cambridge University Press)

Weiss G H 1994 *Aspects and Applications of the Random Walk Amsterdam* (Amsterdam: North-Holland)

Weiss G H, Porrà J M and Masoliver J 1998 The continuous-time random walk description of photon motion in an isotropic medium *Opt. Commun.* **146** 268–76